Journal Pre-proof

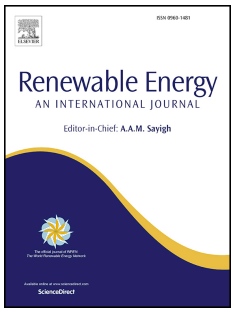

Pyrolysis kinetics of chemically treated and torrefied radiata pine identified through thermogravimetric analysis

Nor Sharliza Mohd Safaai, Shusheng Pang

PII: S0960-1481(21)00637-6

DOI: https://doi.org/10.1016/j.renene.2021.04.117

Reference: RENE 15326

To appear in: *Renewable Energy*

Received Date: 11 August 2020

Revised Date: 14 April 2021

Accepted Date: 22 April 2021

Please cite this article as: Mohd Safaai NS, Pang S, Pyrolysis kinetics of chemically treated and torrefied radiata pine identified through thermogravimetric analysis, *Renewable Energy*, https://doi.org/10.1016/j.renene.2021.04.117.

Credit authorship contribution statement

Nor Sharliza Mohd Safaai: Conceptualization, Experiment and Methodology, Resources, Data curation, Analysis of the results, Writing-original draft, Writing-reviewing and editing

Shusheng Pang: Supervision, Fund, Writing-reviewing and editing

Pyrolysis kinetics of chemically treated and torrefied radiata pine identified through thermogravimetric analysis

Nor Sharliza Mohd Safaai[a,b] and Shusheng Pang[a]

[a]Department of Chemical and Process Engineering, University of Canterbury, Private Bag 4800, Christchurch 8140, New Zealand

[b]Faculty of Chemical Engineering, Universiti Teknologi MARA, 41500 Shah Alam, Selangor, Malaysia

Corresponding author: norsharliza.mohdsafaai@pg.canterbury.ac.nz

Pyrolysis kinetics of chemically treated and torrefied radiata pine identified through thermogravimetric analysis

Nor Sharliza Mohd Safaai[a,b] and Shusheng Pang[a]

[a]Department of Chemical and Process Engineering, Level 4, University of Canterbury, Private Bag 4800, Christchurch 8140, New Zealand

[b]Faculty of Chemical Engineering, Universiti Teknologi MARA, 41500 Shah Alam, Selangor, Malaysia

Corresponding author: norsharliza.mohdsafaai@pg.canterbury.ac.nz

Abstract

This study investigates the effects of separate and combined chemical (acid and alkaline pretreatment) and torrefaction pretreatment of radiata pine biomass on the pyrolysis kinetic parameters using thermogravimetric analysis (TGA). Thermal degradation profiles of the treated biomass samples were examined and correlated to changes in proximate and ultimate analyses. The TGA results were then used to determine the activation energies (E_a) and pre-exponential factors (A) in various kinetic models, including Kissinger, Kissinger-Akahira-Sunose (KAS), Flynn-Wall-Ozawa (FWO), and simplified Distributed Activation Energy Model (DAEM) methods, where the obtained values of E_a for these models ranged between 170.9–270.9 kJ·mol^{-1}, 170.1–262.3 kJ·mol^{-1}, 186.2–259.2 kJ·mol^{-1}, and 169.3–266.3 kJ·mol^{-1}, respectively, for all of the treated biomass samples. The mean E_a values after pretreatments increased in comparison with that of the Control sample. In general, the E_a values increased over the degree of conversion from 0.2 to 0.8 attributed to the crystallinity and carbonisation effects upon pretreatments. However, the mean E_a values varied with the pretreatment methods, indicating a complex multi-step mechanism of pyrolysis process of the treated biomass. The A values determined for all of the treated

biomass samples varied over a broad magnitude ranging from 10^5 to 10^{26} s^{-1} for the adopted kinetic models.

Keywords: Acid pretreatment; Alkaline pretreatment; Torrefaction; Kinetic models; Pyrolysis; Thermogravimetric analysis.

1.0 Introduction

Biomass is an abundant yet underutilised renewable resource composed of cellulose, hemicellulose, and lignin. As a potential resource for bio-oil, biomass pretreatments, such as biological, physical, chemical, and physiochemical processes, have received considerable attention to modify and/or remove hemicellulose and lignin for subsequent conversion process [1]. The continuous investigation of biomass pretreatments have demonstrated a promising step of biomass upgrading before feeding into conversion process to produce the bio-oil with improved quality. It is known that properties of bio-oil derived from pyrolysis of raw biomass exhibits shortcomings, include high oxygen content, water content, and acidity, which retard the economic potential of the bio-oil [2].

Past studies [3-6] have shown that chemical pretreatments can remove alkaline metals, reduce the degree of polymerisation of cellulose while increasing its crystallinity, and facilitate thermal degradation during pyrolysis. However, different pretreatment methods have different impacts on the biomass matrix and the subsequent pyrolysis process. Pretreatment with dilute sulfuric acid is a widely adopted method, since it is economical and can remove undesirable metal elements, thus generating the solid substrate

enriched in cellulose for the pyrolysis [1]. Alkaline pretreatment has also been reported to selectively disrupt lignin structure and partially dissolve hemicellulose without degrading cellulose due to its high degree of polymerisation and high crystallinity [7]. In the alkaline pretreatment, sodium hydroxide is the most effective reagent, and the pretreatment is carried out under mild conditions compared with those required for acid pretreatment [8]. Moreover, alkaline pretreatment can reduce the acidity of bio-oil upon pyrolysis [9, 10] due to the elimination of acidic groups, such as the acetyl and uronic acids [11].

The positive effects of acid and alkaline pretreatments encouraged the exploration of combining these reagents to modify the raw biomass for improving bio-oil quality from pyrolysis. A recent study on sugarcane bagasse found that the cellulose content was increased to 83% from sequential dilute sulfuric acid and dilute sodium hydroxide pretreatments [12]. The combined pretreatments had enabled modification of biomass structure and composition for desired bio-oil quality from the pyrolysis; hence, bio-oil upgrading can be minimised [13]. In addition to chemical pretreatment, torrefaction is also a favourable option for biomass upgrading for the subsequent pyrolysis. This thermal pretreatment occurs between 200 °C–300 °C, which considerably influences the pyrolysis characteristics and kinetics [14, 15]. Recently, combined chemical and torrefaction pretreatments have received attention due to the coupling effects on the changes in biomass structure and composition [16, 17]. Through combined pretreatment, some of the inorganic elements in the raw biomass are removed, and the contents of carboxyl, moisture, and oxygen are reduced [18].

To better understand the impacts of the biomass pretreatment on the pyrolysis performance, there is a need to analyse the effects of pretreatments on biomass structural

and chemical composition changes, thermal behaviour, and pyrolysis kinetic parameters. It is known that activation energy, E_a, and pre-exponential factor, A, are the basic parameters for kinetic analysis using a first-order kinetic model. These parameters could be determined from TGA experiments in predicting the dynamics and behaviours of the feedstock during thermal degradation. Moreover, a reliable kinetic model for biomass pyrolysis is crucial in designing and optimising industrial systems due to the complexity of biomass reaction schemes and the formation of numerous chemical compounds [19].

Extensive studies on kinetic modelling of biomass pyrolysis have been reported in the literature using isoconversional kinetic models [20-23]. For instance, Mishra et al. [20] evaluated the pyrolysis kinetic parameters of raw pinewood using isoconversional plots. Díaz et al. [22] compared the pyrolysis kinetic parameters for raw Canary Island pine using Kissinger and Flynn-Wall-Ozawa (FWO) models. In a separate study, Varma and Mondal [24] determined the pyrolysis kinetic parameters for pine needles, respectively, employing Kissinger-Akahira-Sunose (KAS), Ozawa-Flynn-Wall (OFW), and Coats-Redfern models. It is found that the values of the kinetic parameters varied significantly with the biomass species, TGA operating conditions, and the kinetic models employed. In addition, the pretreatment methods also affect the pyrolysis kinetic parameters. Zhang et al. [25] found that acid/alkaline pretreatments of waste cassava decreased the activation energy and promoted the decomposition in the fast pyrolysis. Similar finding was reported in a separate study on pyrolysis of acid pretreatment of elephant grass [26].

Isoconversional methods have also been used to determine the pyrolysis kinetic parameters for torrefied biomasses [15, 27, 28]. Zhang et al. [29] and Kasim et al. [30] studied the pyrolysis kinetic parameters in pyrolysis of treated biomass with combined acid

leaching and torrefaction. From these studies, it is found that the activation energy was significantly increased with the combined pretreatment. However, the combined alkaline and torrefaction pretreatment of biomass has not been found in the literature and the pyrolysis kinetic parameters of this approach are unknown.

The objectives of this work are to investigate the pyrolysis kinetic parameters of radiata pine biomass subjected to separate or combined acid, alkaline, and torrefaction pretreatments. Pyrolysis experiments were conducted using TGA at different heating rates in nitrogen atmosphere under non-isothermal conditions. Based on the TGA results, pyrolysis performances of the treated biomasses were thoroughly analysed and compared. Finally, four different mathematical models (Kissinger, KAS, FWO, and DAEM) have been applied to the TGA data for evaluating kinetic parameters during pyrolysis.

2.0 Materials and Methods

2.1 Biomass chemical and torrefaction pretreatments

Fresh radiata pine sawdust was obtained from a local sawmill near Christchurch, New Zealand. The biomass was ground into 1–2 mm of particle size and then oven-dried. Subsequently, every 100 g of biomass samples were treated, respectively, using dilute sulfuric acid (H_2SO_4) of 0.1 M and sodium hydroxide (NaOH) of 1.75 M, as described in Table 1. The pretreatment temperature in each case was controlled using a water bath. Deionised water was used as a washing agent to eliminate excess chemicals upon pretreatments. Then, the treated biomass was dried at 105 °C for 24 h and kept in leak-proof container before further use. Combined chemical pretreatment involved alternation of acid and alkaline pretreatment, in which the details are included in Table 1.

Then, the chemically treated biomass samples and untreated (Control) samples were further treated with torrefaction in a lab-scale unit which was similar to that reported elsewhere [31] and illustrated in Figure 1. For each pretreatment and the Control, 100 g of the ground biomass samples were placed in a steel batch reactor, which is fixed inside an electric oven. The reactor was welded with Kleanflow tri ferrule and sealed with Kleanflow tri clamp to avoid gas leakage during the torrefaction [32]. Before heating up, the reactor was purged to displace remaining air with nitrogen at flowrate of 2 SLPM (standard condition litre per minute) and this purge continued for 10 min. The torrefaction was conducted at mild condition of 250 °C in a duration of 30 min.

A K-type thermocouple was placed at the centre of the reactor to monitor and Control the inside temperature with an average heating rate of 1.15 °C·min^{-1}. The vapour from the torrefaction was condensed in a condenser, while the non-condensable gases were exhausted to venting line. Finally, the torrefied biomass was collected, weighed, sealed, and stored at room temperature. The summary of pretreatments employed in this work is presented in Figure 1.

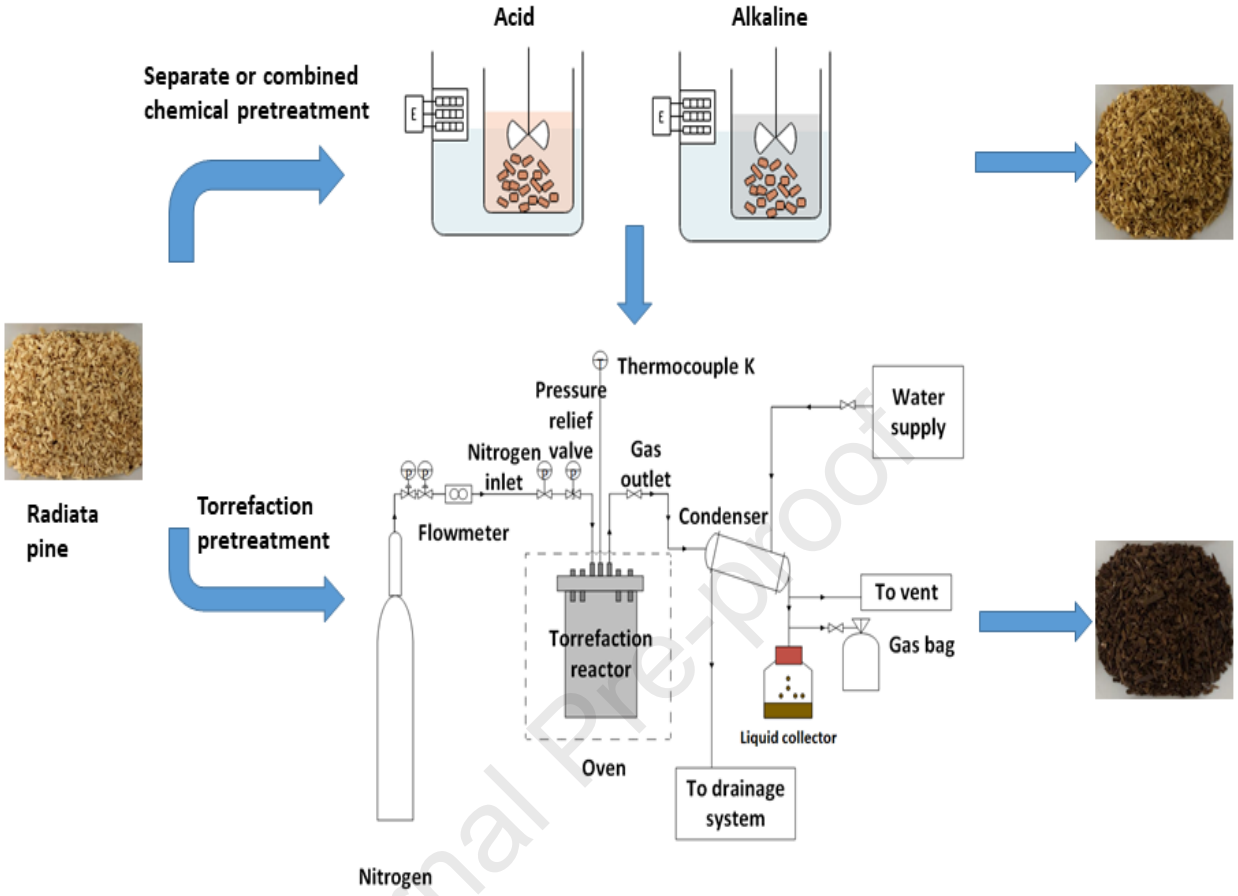

Figure 1: Schematic diagram of radiate pine pretreatment conducted in this work.

Table 1

Biomass pretreatments and operation conditions

Sample number	Sample ID	Pretreatment	Operating condition
1	Control	Untreated	-
2	Acid treatment (AC)	0.1 M H_2SO_4	50 °C (2 h)
3	Alkaline treatment (AL)	1.75 M NaOH	70 °C (2 h)
4	Combined acid and alkaline pretreatment (ACAL)	0.1 M H_2SO_4 and 1.75 M NaOH	50 °C (2 h) and 70 °C (2 h)
5	Combined alkaline and	1.75 M NaOH and	70 °C (2 h) and

	acid treatment (ALAC)	0.1 M H_2SO_4	50 °C (2 h)
6	Torrefaction pretreatment (TO)	Torrefaction	250 °C (30 min)
7	Combined acid and torrefaction pretreatment (ACTO)	0.1 M H_2SO_4 and torrefaction	50 °C (2 h) and 250 °C (30 min)
8	Alkaline and torrefaction pretreatment (ALTO)	1.75 M NaOH and torrefaction	70 °C (2 h) and 250 °C (30 min)
9	Combined acid, alkaline and torrefaction pretreatment (ACALTO)	0.1 M H_2SO_4, 1.75 M NaOH and torrefaction	50 °C (2 h), 70 °C (2 h) and 250 °C for 30 min
10	Combined alkaline, acid and torrefaction pretreatment (ALACTO)	1.75 M NaOH, 0.1 M H_2SO_4 and torrefaction	70 °C (2 h), 50 °C (2 h) and 250 °C for 30 min

137

138 **2.2 Elemental analysis**

139 The mass contents of carbon, hydrogen, oxygen and nitrogen of the Control and the
140 treated biomass samples were determined through complete oxidation with the elementary
141 analyser, in accordance with ASTM D5373. The oxygen content was calculated by the
142 difference on a dry-ash free basis. The contents of moisture, ash and volatile were
143 determined based on the procedure ISO 11722, ASTM D1102 and ISO 562, respectively,
144 while the fixed carbon was obtained by difference.

145

146 **2.3 TGA and DTG analysis**

147 TGA of the radiata pine samples was performed in a thermogravimetric analyser
148 (NETZSCH STA 449 F3) under nitrogen atmosphere. In each experimental run, the
149 analyser was first purged with nitrogen, and then 10 mg of wood sample was loaded in an
150 alumina crucible. The sample was heated up from ambient temperature to 800 °C at heating

rates of 10, 20 and 30 °C min^{-1}, respectively, with a constant nitrogen flow rate of 20 ml min^{-1}. The data obtained were used for kinetic analysis.

2.4 Kinetic analysis and determination of the kinetic parameters

In biomass pyrolysis, the biomass is first thermally decomposed and then the derived compounds may undergo cracking and re-polymerisation from which non-condensable gases, bio-oil vapours and char are produced. Different reactions occur at different stages and the pyrolysis mechanism is complex, therefore, isoconversional modelling can be used to quantitatively describe the biomass pyrolysis process [19]. This type of models contains parameters of activation energy and pre-exponential factor which can be fitted from the experimental results at different temperatures and heating rates, thus the model can be applied in a broad range conditions. Uncertainties induced by the experimental errors and from the fitting the kinetic parameters can be minimised by describing the complex process in the form of a functional dependence of activation energy on the degree of conversion [33].

In analysis of the reaction kinetics, the general rate equation for the heterogeneous solid-state pyrolysis under a non-isothermal condition can be expressed by the following canonical equation:

$$\frac{d\alpha}{dt} = k(T)f(\alpha) \quad (1)$$

where α signifies the degree of conversion, and $d\alpha/dt$ denotes the conversion rate. α can be calculated using Eq. (2):

$$\alpha = \frac{W_o - W_t}{W_o - W_\infty} \quad (2)$$

where W_o, W_t and W_∞ refer to the mass of substrate at the initial state, at time *t*, and at the final state, respectively.

k(T) in Eq.(1) represents as the reaction rate constant and can be expressed by the Arrhenius equation with the form of:

$$k(T) = A\ exp\left(-\frac{E_a}{RT}\right) \quad (3)$$

In which E_a is the apparent activation energy or simply the activation energy (kJ·mol^{-1}), *A* is the pre-exponential factor (s^{-1}), R is the gas constant (J K^{-1}mol^{-1}), and *T* is the pyrolysis temperature (K). Therefore, Eq. (1) can be re-written as:

$$\frac{d\alpha}{dt} = A\ exp\left(-\frac{E_a}{RT}\right) f(\alpha) \quad (4)$$

The function $f(\alpha)$ is used for describing solid-state first order reaction which can be determined by:

$$f(\alpha) = (1-\alpha)^n \quad (5)$$

where n is the reaction order. Substituting Eq. (4) into Eq. (5) generates the expression of reaction rate as shown in Eq. (6):

$$\frac{d\alpha}{dt} = A\ exp\left(-\frac{E_a}{RT}\right).(1-\alpha)^n \quad (6)$$

For non-isothermal TG analysis at constant heating rate, β, the following equation can be derived from Eq. (6):

$$\frac{d\alpha}{dT} = \frac{A}{\beta}\ exp\left(-\frac{E_a}{RT}\right) f(\alpha) \quad (7)$$

Where $\beta = dT/dt = (dT/d\alpha)\ (d\alpha/dt)$.

The above equation expresses the fraction of material transformed as a function of time and reaction temperature. The function *f(α)* in Eq. (7) can be expressed by different formulas depending on the reaction mechanisms.

In this work, the non-isothermal TGA experimental results were used and only the activation energy, E_a, and pre-exponential factor, *A*, were determined. The methods used to calculate these kinetic parameter are called model-free non-isothermal methods and require experiments to be carefully designed at different reaction temperatures and heating rates.

2.5 Model-free isoconversional methods to identify the kinetic parameters

The model-free methods allow to obtain the kinetic parameters of a solid-state reaction without knowing the reaction mechanism. In this study, four different models were employed and corresponding kinetic parameters were determined and analysed.

2.5.1 Kissinger model

At the peak temperature (T_{peak}), where the maximum rate of decomposition is reached, the second derivative of Eq. (4) is equal to zero and is given by Eq. (8).

$$\frac{d^2\alpha}{dt^2} = \left[\left(\frac{E_a\beta}{RT^2{}_{peak}}\right) + A\, exp\left(-\frac{E_a}{RT_{peak}}\right) f'(\alpha)\right]\frac{d\alpha}{dt} = 0 \quad (8)$$

Where $f'(\alpha)$ is the first order derivative of $f(\alpha)$. After rearrangement, Eq. (8) becomes:

$$\frac{\beta}{T^2{}_{peak}} = \left(\frac{AR}{E_a}\right) exp\left(\frac{-E_a}{R}\right) f'(\alpha) \quad (9)$$

By taking natural log on both sides, Eq. (9) is changed to linear regression as follows:

$$ln\left(\frac{\beta}{T^2{}_{peak}}\right) = \left(\frac{-E_a}{R}\right)\left(\frac{1}{T_{peak}}\right) + ln\left(\frac{AR}{E_a}\right)n(1-\alpha)^{n-1} \quad (10)$$

The activation energy can be fitted from a plot of $\ln(\beta/T_{peak}^2)$ against $1/T_{\text{peak}}$ from Eq. (10) for a series of experiments at different heating rates (β), where T_{peak} is the peak temperature of the DTG curve. The activation energy, E_{a} can be calculated from the slope of the function, which is equal to $-E_{\text{a}}/\text{R}$.

In this study, it is assumed that biomass pyrolysis is a first-order reaction in which n = 1. Though it is not always the case, the simplicity and the number of parameters of the first-order model allow the direct comparison of different fuels to provide estimation of parameters for further and more accurate modelling. Therefore, Eq. (10) can be simplified to the following form:

$$ln\left(\frac{\beta}{T^2peak}\right) = \left(-\frac{E_a}{R}\right)\left(\frac{1}{T_{peak}}\right) + ln\left(\frac{AR}{E_a}\right) \quad (11)$$

2.5.2 Kissinger-Akahira-Sunose (KAS) model

The KAS model takes into account the variation of activation energy with reaction temperature and employs the Arrhenius equation for integration over a range of temperatures from the initial value, T_o, to the given temperature, T, in the experiments.

$$g(x)\int_0^{\alpha}\frac{d_\alpha}{f(\alpha)} = \frac{A}{\beta}\int_{T_0}^{T} exp\left(-\frac{E_a}{RT}\right)dT = \frac{AE_a}{\beta R}\mathcal{P}\left(\frac{E_a}{RT}\right) \quad (12)$$

The KAS equation uses the following approximation of $\mathcal{P}\left(\frac{E_a}{RT}\right)$ which is given by Coats and Redfern [34] as follows:

$$\mathcal{P}\left(\frac{E_a}{RT}\right) \cong \frac{exp\left(\frac{E_a}{RT}\right)}{\left(\frac{E_a}{RT}\right)^2} \quad (13)$$

On substitution of Eq. (10) into Eq. (9) and further simplification by linearisation, the KAS equation is obtained as

$$ln\left(\frac{\beta_i}{{T_{\alpha,i}}^2}\right) = ln\left(\frac{A_\alpha R}{E_{a,_\alpha} g_\alpha}\right) - \frac{E_{a,\alpha}}{RT_{\alpha,i}} \quad (14)$$

E_a can be determined from Eq. (15) by plotting $ln\left(\frac{\beta_i}{{T_{\alpha,i}}^2}\right)$ versus $\frac{1}{T_{\alpha,i}}$ for each value of conversion, α, at different heating rates. Subscript *i* in Eq. (15) denotes the heating rate at which the non-isothermal TGA runs are operated. $T_{\alpha,i}$ represents the temperature at the *i* heating rate and corresponding conversion, α.

2.5.3 Flynn-Wall-Ozawa (FWO) model

The Flynn-Wall-Ozawa (FWO) model uses Doyle's approximation for estimation of temperature integral when integrating Eq. (4). Based on this mode, Eq. (15) is obtained as follow:

$$ln\beta_i = ln\left(\frac{A_\alpha R}{E_{a,\alpha} g(\alpha)}\right) - 5.331 - 1.052\frac{E_{a,\alpha}}{RT_{\alpha,i}} \quad (15)$$

From the above equation, $E_{a,\alpha}$ can be computed from the slope of $\ln\beta_i$ versus $1/T_{\alpha,i}$ in the curves plotted from experimental results for each heating rate with corresponding value of α. In this way, E_a can be determined from the TGA curves without assumption of reaction order, while *A* can be determined using thermodynamic equation [35] as the following:

$$A = \beta E_a exp\left(\frac{E_a}{RT_p}\right)/\left(RT_p^2\right) \quad (16)$$

2.5.4 Simplified Distributed Activation Energy Model (DAEM)

This model assumes that all the reactions of a particular family share the same pre-exponential factor and that the activation energy triggered by any reaction can be represented by a distribution function [36]. The DAEM is employed in the following form for determination of mass change of solid to volatiles [37]:

$$1 - \alpha = \int_0^\infty exp\left(-A \int_0^t e^{-E_a/RT}\, dt\right) f(E)dE \quad (17)$$

Where α is the total conversion of decomposition reaction at temperature T, $f(E)$ is the normalised distribution function of the activation energies of the multiple first-order irreversible reactions, β is the linear heating rate of the decomposition reaction, and A is the pre-exponential factor. A simple integral method was developed by Miura and Maki [38] for calculation of E_a and A from three sets of experimental data obtained at different heating rates. The working form of Arrhenius equation can be described as follows:

$$ln\left(\frac{\beta}{T^2}\right) = ln\left(\frac{AR}{E_a}\right) + 0.6075 - \left(\frac{E_a}{R}\frac{1}{T}\right) \quad (18)$$

This model provides a straightforward method in estimating E_a and A values from Arrhenius plot of ln (β/T^2) versus 1/T at selected α for three different heating rates. The values of E_a and A can be obtained from the slope and the intercept in each Arrhenius curve, respectively.

3.0 Results and Discussion

3.1 Biomass properties of Control and treated biomass samples

Table 2 summarises the results obtained from proximate and ultimate analysis of the Control, treated biomass samples of radiata pine in the present study and those of lodgepine from literature. The results show that all treated biomass samples had low moisture content of less than 10%, thus were favourable for the subsequent pyrolysis. In general, ash content was reduced with the pretreatment, particularly with acid pretreatment, which removed some of the inherent inorganic salts. However, the ash content after NaOH pretreatment was increased which was attributed to the deposit of Na-based compounds from the alkaline reagent on the biomass. This result is in agreement with the finding in previous study on alkaline pretreatment of wheat straw and barley using 1%–2% NaOH [39]. It is also observed that the ash contents of the torrefied biomass was slightly increased, which agreed with the result reported on torrefaction of *Pinus Patula* wood from 0.26% to 0.28% [40].

Table 2.

Results of proximate and ultimate analysis of Control and treated biomass samples.

	Proximate analysis				Ultimate analysis			
Type of biomass	Moisture (%)	Ash (%)	Volatile (%)	Fixed Carbon (%)	Carbon (%)	Hydrogen (%)	Nitrogen (%)	Oxygen (%)
Control	2.30	0.40	82.20	15.10	48.90	6.07	0.06	42.30
AC	1.90	0.13	80.20	14.90	47.40	5.77	0.05	40.80
AL	1.80	1.10	76.80	20.30	48.50	6.01	0.07	42.50
ACAL	1.60	1.10	76.60	20.70	48.70	6.01	0.04	42.60
ALAC	1.70	0.02	85.70	12.60	49.10	6.05	0.05	42.10
TO	2.80	0.43	73.70	23.10	52.50	5.74	0.04	38.40
ACTO	2.60	< 0.1	76.10	21.30	52.20	5.69	0.02	39.50
ALTO	2.70	1.00	75.40	20.90	50.80	5.81	0.05	39.70

ACALTO	2.40	0.97	74.60	22.00	51.20	5.70	0.01	39.80
ALACTO	2.50	1.10	72.90	23.50	52.60	5.71	0.04	38.00
Lodgepole pine **[41]***	4.20	0.69	80.23	15.10	52.23	6.20	0.47	41.23

*Note: The literature data are included for comparison.

According to Park et al. [42], the ash content increased in the torrefied biomass is caused by the thermal break-up of carbohydrates fractions, resulting in the build-up of residual ash after torrefaction. In the present study, it is also found that the pretreatments maintained a high content of volatile matters (72.9–85.7%) and a low ash content (< 0.1–1.1%) in the treated biomasses, indicating an easy ignition fuel [37]. The Control sample had volatile content of 82.15 and ash content of 0.4%. The treated biomass samples had fixed carbon contents ranging from 12.6% to 23.5% in comparison with 15.1% for the Control sample. The samples subjected to torrefaction tended to have higher contents of fixed carbon and lower content of volatiles.

Results from ultimate analysis revealed the carbon content changes were insignificant (less than 1.5%) for the chemically treated biomasses, varying from 47.7 to 49.1% in comparison with 48.9% for the Control sample. However, the carbon content was significantly increased for the samples after torrefaction (50.8% to 52.6%). The results also show that the hydrogen and oxygen contents were decreased for all of the torrefied samples and these results are consistent with those in previous studies on biomass torrefaction [23, 40, 43]. For chemically treated samples, a trend of slight decrease in hydrogen content was observed, whereas the oxygen content maintained relatively constant. These patterns were also found in previous studies on acid and alkaline pretreatments of the biomass [10, 16, 44, 45]. However, one previous study showed a decreasing trend in oxygen content with acid pretreatment of the Napier grass biomass [10]. It is interesting to note that the nitrogen

content was significantly reduced from 0.06% to a range between 0.01 and 0.05% with torrefaction pretreatment, indicating lowered NOx from pyrolysis of treated samples.

3.1 Thermal decomposition behaviour of Control and treated biomasses through the TG analysis

Fig. 2 (a) and (b) show the pyrolysis thermal behaviours for various treated biomass samples at a fixed heating rate of 30°C·min^{-1} through the TG analysis. As can be observed in the TG curves, the thermal decomposition of biomass can be divided into three distinct stages based on the TG curve shapes [20, 46] in the temperature range between 50 °C and 800 °C. Stage I occurs from 50 °C to 150 °C, in which the weight loss is associated with the evaporation of bound water adsorbed in the wood substance. With further increase in the operation temperature in Stage II, the biomass pyrolysis begins and continues over the temperature range of 245 °C to 540 °C. In Stage II, the rate of weight loss is increased. A sharp increase in weight loss is observed in the temperature range from 300 °C to 400 °C. This trend is attributed to volatile hydrocarbon production from the decomposition of hemicelluloses, cellulose and, to a less extent, the decomposition of lignin [47].

TG curves in Fig. 2 (a) reveal that the pretreatments had significantly affected the degradation process despite all samples showing a similar pattern. Fig. 2 (b) illustrates a noticeable hemicellulose shoulder for AC sample, indicating the retaining of hemicellulose after acid pretreatment. A similar shoulder with less intensity was observed for the AL sample, suggesting that the decomposition of hemicellulose during the alkaline pretreatment was more remarkable than that in the acid pretreatment. This result is

inconsistent with previous study upon biomass pretreatment with 1% H_2SO_4 and 1% NaOH [48], which may be due to the difference of reagent's severity in the pretreatments. Subsequent to combining the chemical pretreatments of the biomass (ACAL and ALAC), the shoulder disappeared, implying that the hemicellulose was massively removed during the pretreatments.

Hemicellulose shoulder was also found to have vanished after being subjected to torrefaction, which can be explained by further removal of hemicellulose during the pretreatment [40]. It is reported that at lower range of pyrolysis temperatures, the hemicellulose decomposes faster than cellulose due to its linear polymer structure with short side chains [49]. In contrast, cellulose molecules contain mainly long polymer chains of glucose units with crystalline and sturdy, making it difficult to degrade [50]. Lignin is composed of polysaccharides which are strongly cross-linked and thermally stable. Thus, lignin leads to decompose in a broader range of temperatures between Stage II and Stage III [49]. The thermal stability of samples was slightly increased upon torrefaction pretreatment due to decreased content of volatile matter in the torrefied biomass [40].

As shown in DTG curves, biomass with different pretreatment exhibits different peak values, which are proportional to the biomass reactivity and the physicochemical properties [49, 51]. Based on the peak values, the AC sample has the highest reactivity, and the reactivity of all samples follows the order of AC > ACTO > TO > ALAC > ACALTO > ALTO > ALACTO > AL > Control > ACAL. According to a study by Eom et al. [52], the increase in peak value is linked to the increase in cellulose thermal stability, which was observed for acid treated biomass [53].

The chemical and torrefaction pretreatments had significant influence on the peak temperature, T_{peak}. The T_{peak} value corresponds to the maximum decomposition rate of the hemicellulose and the cellulose components in the biomass. All samples exhibited a reduced T_{peak} value ranging between 347 °C and 380 °C compared with the Control sample (381 °C). The T_{peak} value is also linked to the demineralisation effect of the pretreatments, which reduces the contents of alkali and alkaline earth metallic (AAEM) species [54]. In the present study, the lower T_{peak} values for AL (349°C), ACAL (347°C), and ALAC (373°C) treated biomass samples are linked to the introduced AAEMs to the biomass through ion-exchange after alkaline pretreatment [48]. The AAEMs promote cellulose decomposition at low temperatures through a modification of the degradation mechanism [55]. Therefore, the T_{peak} value was reduced in comparison to the Control sample (381°C). AC sample recorded T_{peak} value of 369 °C although most of the AAEMs were effectively removed [55, 56]. This shift to low temperature could be linked to the high stability of hemicellulose upon removal of side groups (acetyl groups), thus, it was decomposed at a similar temperature as the cellulose [57].

Similar trend of T_{peak} values was observed for all samples treated with torrefaction, which mildly shifted toward lower temperatures ranging from 371 °C to 380 °C. The slight reduction of T_{peak} indicates that the structural characteristics of the cellulose fraction of the biomass were preserved after the torrefaction treatment, which is consistent with the finding in a past study [40]. However, the T_{peak} of the combined pretreatment of ALACTO shifted to a much lower value of 366 °C. This could be linked to the highest ash content (1.10%) with the ALACTO pretreatment, which acts as a catalyst during thermal degradation [56].

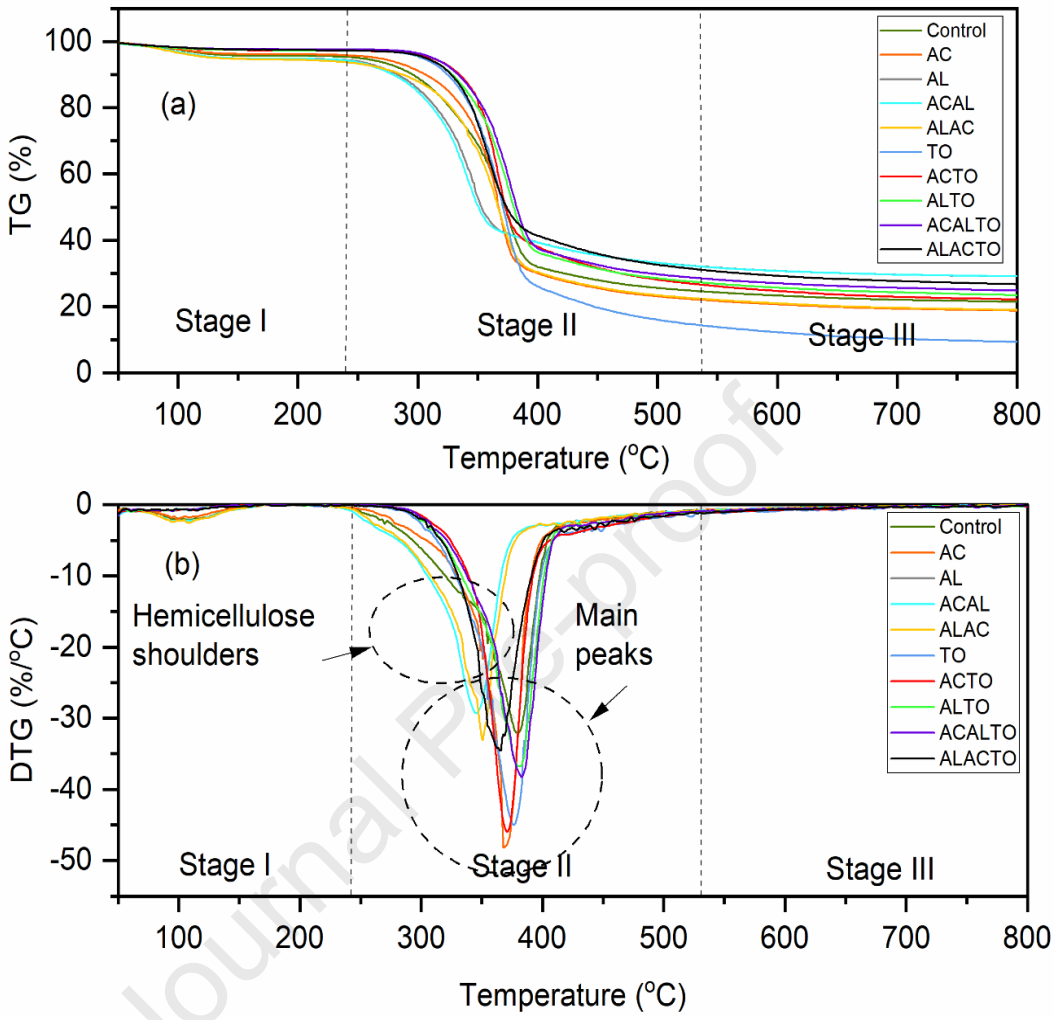

Fig.2: TG and DTG curves of biomass samples at a heating rate of 30°C·min^{-1}

Fig. S1(i) and (ii) depict the TG and DTG curves of Control and treated samples at heating rates of 10 °C·min^{-1}, 20 °C·min^{-1}, and 30 °C·min^{-1}. From Fig. S1 (i) (a), it is observed that a significant weight loss of the Control biomass occurred from 250 °C to 430 °C, responding to the hemicellulose and cellulose degradation. The heating rate did not have a statistically significant effect on the biomass decomposition pattern. However, with the increasing heating rate, the initial decomposition rate was slightly lower, and the fast

decomposition starting point shifted to higher temperatures. The initial slow decomposition rate was due to the heat transfer limitations [22]. A higher heating rate tended to enhance the reaction rate in the same temperature region. Therefore, a higher temperature was required to achieve a fast rate of biomass decomposition.

It is observed that all treated samples illustrated similar TG and DTG profiles (Fig. S1). However, the T_{peak} values varied with different pretreatment methods and heating rates. Additionally, the start and final temperatures of each stage changed due to structural changes upon the pretreatments. As an example for the AC sample, the T_{peak} value shifted from 353 °C to 363 °C and then to 369 °C when increasing the heating rate from 10 °C·min^{-1} to 20 °C·min^{-1} and then to 30 °C·min^{-1}, respectively. The pattern observed from this study is in agreement with the results from studies on pinewood pretreatment [23, 37]. Similarly, the torrefied biomass (ACTO) also showed T_{peak} values shifted from 362 °C to 365 °C and then to 371°C at the above heating rates.

3.2 Determination of kinetic parameters by Kissinger, KAS, FWO, and DAEM methods

The data derived from TG and DTG curves were utilised to determine the kinetic parameters for biomass decomposition to represent the biomass slow pyrolysis. The kinetic parameters included apparent activation energy, E_a, and pre-exponential factor, A, based on Kissinger, KAS, FWO, and DAEM models. The computed results are presented in Table 3 for Control and the treated biomass samples. Overall, the activation energy agrees closely with the results reported in the literature (195–286 kJ·mol^{-1}) for cellulose decomposition, which is paramount for pyrolysis [58].

Table 3.

The average values of kinetic parameters determined using Kissinger, KAS, FWO, and DAEM models for Control and the treated biomass samples

Biomass	Activation energy, E_a (kJ·mol^{-1})				Exponential factor, A (s^{-1})			
	Kissinger	KAS	FWO	DAEM	Kissinger	KAS	FWO	DAEM
Control	170.7	190.1	197.1	198.2	6.1×10^{10}	1.0×10^{11}	2.3×10^{11}	2.8×10^{18}
AC	271.0	237.6	245.7	246.9	2.8×10^{19}	8.7×10^{12}	2.5×10^{13}	6.7×10^{21}
AL	170.9	170.1	186.2	169.3	4.5×10^{10}	3.6×10^{13}	5.7×10^{16}	2.1×10^{18}
ACAL	161.3	188.2	192.7	194.9	5.7×10^{10}	5.0×10^{12}	3.6×10^{12}	1.4×10^{23}
ALAC	238.0	234.9	244.0	243.0	4.1×10^{16}	1.9×10^{13}	1.6×10^{14}	36×10^{23}
TO	244.2	240.8	240.2	237.2	2.5×10^{5}	4.0×10^{12}	3.3×10^{12}	7.7×10^{21}
ACTO	252.7	227.8	228.3	227.8	2.6×10^{5}	2.5×10^{12}	1.8×10^{12}	3.1×10^{22}
ALTO	242.6	238.7	239.2	242.6	2.5×10^{5}	1.4×10^{13}	4.4×10^{12}	1.2×10^{26}
ACALTO	174.1	215.4	216.6	206.6	1.8×10^{5}	8.4×10^{10}	1.1×10^{11}	6.2×10^{19}
ALACTO	179.9	262.3	259.2	266.3	1.8×10^{5}	4.4×10^{13}	2.8×10^{13}	2.1×10^{25}

For the Kissinger method, linear regression graphs were plotted using Eq. (8). The mean values of E_a and A for the Control sample were 170.7 kJ·mol^{-1} and 6.1×10^{10} s^{-1}, respectively. These values were chosen as reference values for comparison of all treated samples using the Kissinger method. Among the chemically treated samples, the ACAL sample showed the least values for E_a and A, which were 161.3 kJ·mol^{-1} and 5.7×10^{10} s^{-1}, respectively. Correspondingly, the ACAL sample presented the lowest T_{peak} value. However, the ALAC sample showed increased values of E_a and A at 238.0 kJ·mol^{-1} and 4.1×10^{16} s^{-1}, respectively, but the ALAC sample had a higher T_{peak} value than that in ACAL sample. It was found that the AC sample had the highest values of E_a (271.0 kJ·mol^{-1}) and A (2.8×10^{10} s^{-1}), which was likely attributable to the increase in cellulose thermal stability after the acid pretreatment [52]. It is also reported that the transformation of cellulose to active-cellulose induced had increased in the activation energy [59].

For the combined chemical and torrefaction pretreatments, the E_a values were increased to a range between 174.1 and 252.7 kJ·mol^{-1}, while the A values were

414 significantly reduced between 1.8 and 2.6×10^5 s^{-1}. These results indicate that the
415 pretreatments had altered the chemical components of the biomass, thus changing the
416 biomass stability when it is heated. This finding is in agreement with a previous study on
417 poplar wood that thermal pretreatment had enhanced the wood stability and delayed the
418 degradation of wood based on the TG analysis [60]. The chemical stability of a compound
419 is positively correlated to the activation energy value.

420 From the above discussion, the determined values for A varied in an order of five,
421 reflecting that the pyrolysis process was oversimplified using the Kissinger method, which
422 does not take the degree of conversion (α) into account. Therefore, more comprehensive
423 models such as FWO, KAS, and DAEM methods were employed using Eqs. (14), (15), and
424 (18), respectively, for further kinetics elucidation. The results are given in Table 3.

425 From Table 3, it is noticed that each fitting line displays a highly significant
426 correlation with $R^2 > 0.96$. The average values of E_a for the Control biomass sample were
427 190.1 kJ·mol^{-1}, 197.1 kJ·mol^{-1}, and 198.2 kJ·mol^{-1}, respectively, based on the KAS, FWO,
428 and DAEM methods. The corresponding A values ranged from 10^{11} to 10^{18} s^{-1}. These
429 values were greater than those estimated from the Kissinger method (170.7 kJ·mol^{-1} for E_a
430 and 6.1×10^{10} s^{-1} for A). The values of kinetic parameters determined in this work for the
431 Control sample are close to those reported in the literature on pine sawdust by Mishra and
432 Mohanty [37]. In their study, the mean values of activation energy were 171.7, 179.3, and
433 206.6 kJ·mol^{-1} for KAS, FWO, and DAEM methods, respectively, based on the degree of
434 conversion (α) from 0.1 to 0.7.

In this study, the mean activation energies derived from KAS, FWO and DAEM methods were increased after torrefaction pretreatment. This observed pattern is consistent with previous study on combined demineralisation and torrefaction pretreatment of rice husk, which is due to the cross-linking and charring reactions [29]. However, ACTO sample demonstrated lower activation energy than those of AC sample. This could be linked to the stronger structure of AC than ACTO due to high crystallinity of active-cellulose retained after acid pretreatment [59].

It is also observed that the average activation energy derived from KAS and FWO methods showed a discrepancy of less than 10%. This finding is in line with those reported in the literature [61, 62]. Moreover, the mean E_a values derived from the DAEM model showed a low deviation of less than 10% in comparison with the FWO and the KAS models, confirming the reliability of isoconversional kinetic models.

Figs. 3–5 show the graphical plots of β function against $1/T$ for Control, AC, and ACTO samples to determine the kinetic parameters based on KAS (Fig. 3), FWO (Fig. 4) and DAEM (Fig. 5) models. Table 4 portrays the corresponding fitting results and significance (R^2). Similar plots of other treated biomass samples are illustrated in Figs. S2–S4, where the corresponding fitting results and significance (R^2) are tabulated in Table S1.

Table 4 demonstrates that in the range of degree of conversion (α) from 0.2 to 0.8, the correlations were all significant with R^2 greater than 0.9. However, weak correlation was observed outside this range of α. In a separate study on pinewood, significant correlation was reported in the range of degree of conversion from 0.1 to 0.7 [23].

456 According to the iso-conversion plots based on KAS, FWO, and DAEM models, the
457 fitted results of the kinetic parameters (Table 4) demonstrated a general trend of E_a
458 increasing with the degree of conversion from 0.2 to 0.6, which is most likely ascribed to
459 the occurrence of endothermic reactions. However, the fitted E_a values showed a decreasing
460 trend when the degree of conversion is at and beyond 0.6, indicating the occurrence of
461 exothermic reactions [63]. It is worth noting that a reaction with high activation energy has
462 a lower reaction rate at a given temperature due to the complex reaction schemes with
463 parallel, complex, and competitive reactions under an inert atmosphere [64].
464
465

466

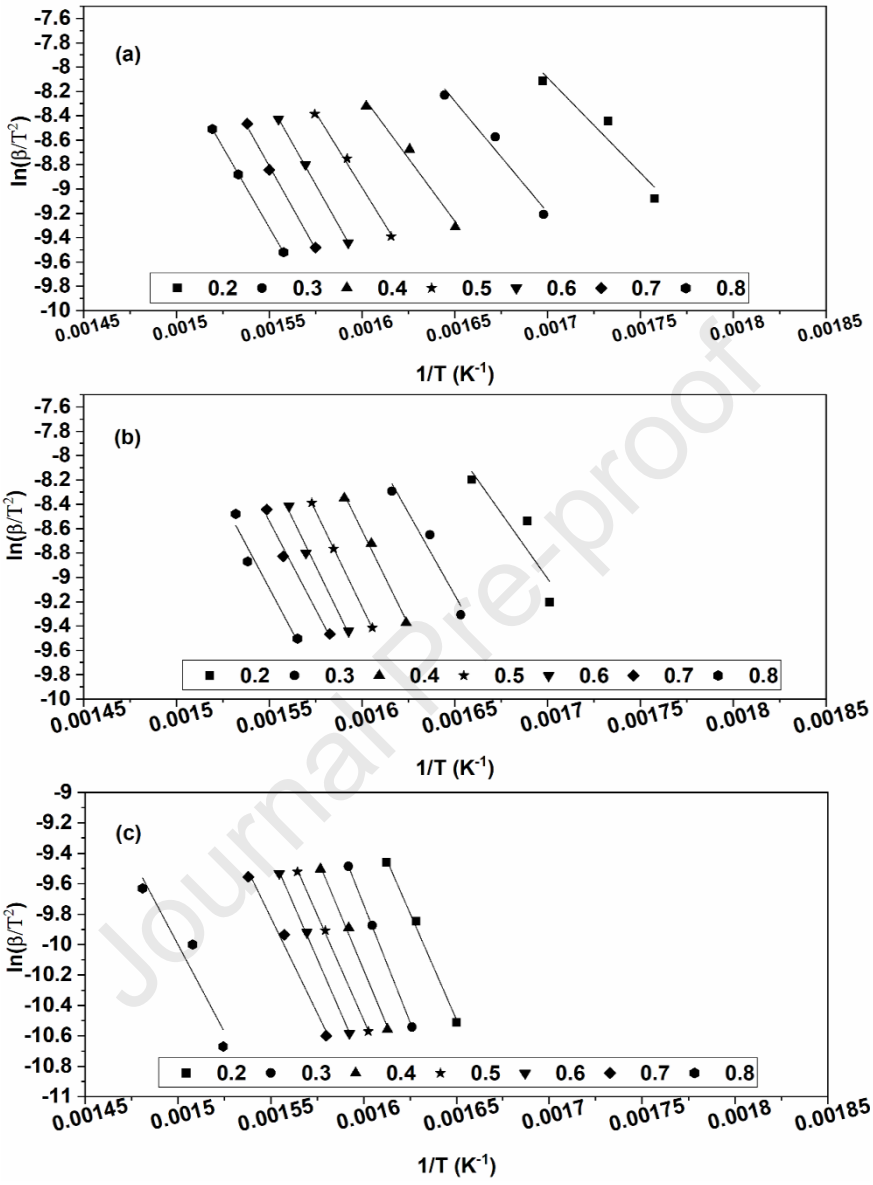

467

468 **Fig. 3.** Plots of ln(β/T^2) against 1/T for determination of kinetic parameters using KAS

469 method for: (a) Control sample; (b) AC biomass; and (c) ACTO biomass at a degree of

470 conversion from 0.2 to 0.8.

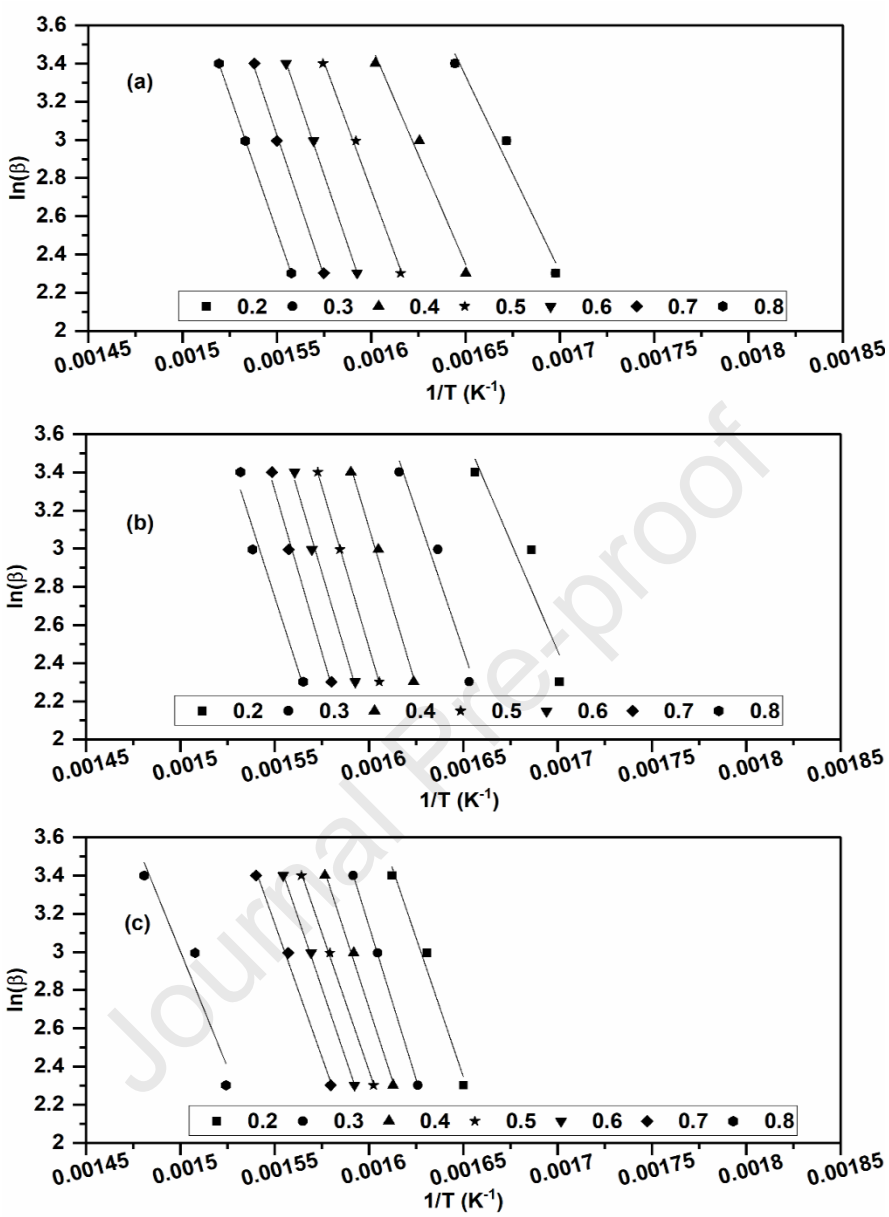

Fig. 4. Plots of ln(β) against 1/T for determination of kinetic parameters using FWO method for: (a) Control sample; (b) AC biomass; and (c) ACTO biomass at a degree of conversion from 0.2 to 0.8.

The activation energies determined using the KAS model for Control, AC, and ACTO samples were in the ranges of 129.8–227.2 kJ·mol^{-1}, 179.0–261.9 kJ·mol^{-1}, and

191.0–256.9 kJ·mol^{-1}, whereas the corresponding values from the FWO model were slightly higher than that from the KAS model, which fell in the ranges of 133.3–233.6 kJ·mol^{-1}, 181.5–269.1 kJ·mol^{-1}, and 192.1–254.0 kJ·mol^{-1}. The fitted activation energy values from DAEM model for Control, AC, and ACTO samples were in the same ranges as the above two models, which were 130.1–235.1 kJ·mol^{-1}, 196.8–269.9 kJ·mol^{-1}, and 191.0–256.9 kJ·mol^{-1}, respectively.

Table 4

Fitted activation energies (kJ·mol^{-1}), pre-exponential factors (s^{-1}), and the correlation coefficients derived from KAS, FWO, and DAEM models for Control, AC, and ACTO biomass samples

Sample	α	KAS			FWO			DAEM		
		E_a (kJ·mol^{-1})	A (s^{-1})	R^2	E_a (kJ·mol^{-1})	A (s^{-1})	R^2	E_a (kJ·mol^{-1})	A (s^{-1})	R^2
Control	0.2	129.8	1.5×10^{6}	0.9232	133.3	2.3×10^{6}	0.9292	130.1	2.7×10^{11}	0.9191
	0.3	151.9	2.5×10^{7}	0.9668	161.8	8.7×10^{7}	0.9734	168.6	2.9×10^{14}	0.9570
	0.4	172.1	3.2×10^{8}	0.9782	181.0	9.8×10^{8}	0.9822	180.2	1.2×10^{15}	0.9801
	0.5	204.7	1.9×10^{10}	0.9953	212.1	4.9×10^{10}	0.9960	212.8	3.3×10^{17}	0.9956
	0.6	225.2	2.5×10^{11}	0.9995	231.6	5.5×10^{11}	0.9996	233.1	9.6×10^{18}	0.9995
	0.7	227.2	3.2×10^{11}	0.9968	233.6	7.1×10^{11}	0.9973	235.1	8.3×10^{18}	0.9970
	0.8	219.6	1.2×10^{11}	0.9999	226.5	2.9×10^{11}	1.0000	227.5	1.2×10^{18}	1.0000
AC	0.2	179.0	7.7×100^{8}	0.8275	181.5	1.1×10^{9}	0.8875	196.8	1.2×10^{17}	0.8933
	0.3	225.0	2.4×10^{11}	0.9508	231.3	5.6×10^{11}	0.9577	219.4	3.7×10^{18}	0.9709
	0.4	257.7	1.4×10^{13}	0.9929	262.5	2.7×10^{13}	0.9939	265.8	1.6×10^{22}	0.9933
	0.5	261.9	2.4×10^{13}	0.9999	266.5	4.5×10^{13}	0.9999	269.9	2.0×10^{22}	0.9999
	0.6	260.1	1.9×10^{13}	0.9897	264.9	3.6×10^{13}	0.9910	268.1	8.9×10^{21}	0.9903
	0.7	241.6	1.9×10^{12}	0.9842	269.1	6.1×10^{13}	0.9910	262.7	2.0×10^{21}	0.9668
	0.8	238.1	1.2×10^{12}	0.9579	244.0	2.7×10^{12}	0.9636	245.9	4.9×10^{19}	0.9605
ACTO	0.2	232.5	6.2×10^{11}	0.9961	229.7	4.4×10^{11}	0.9805	232.5	3.2×10^{21}	0.9961
	0.3	256.9	1.3×10^{13}	0.9999	254.0	9.1×10^{12}	0.9999	256.9	2.0×10^{23}	0.9999

0.4	243.5	2.4×10^{12}	0.9965	241.3	1.9×10^{12}	0.9965	243.5	9.4×10^{21}	0.9961
0.5	229.6	4.4×10^{11}	0.9992	228.3	3.7×10^{11}	0.9993	229.6	4.5×10^{20}	0.9992
0.6	232.6	6.3×10^{11}	0.9992	231.2	5.3×10^{11}	0.9993	232.7	6.0×10^{20}	0.9992
0.7	208.6	3.2×10^{10}	0.9876	221.2	1.5×10^{11}	0.9952	208.6	4.0×10^{18}	0.9876
0.8	191.0	3.5×10^{9}	0.9098	192.1	4.0×10^{9}	0.9187	191.0	3.6×10^{16}	0.9098

In a raw pine sawdust study by Xiao et al. [65], the DEAM model was employed, where a significant linear relationship was observed between the β function and $1/T$. However, the activation energy obtained in their study (245.8 kJ·mol^{-1}) was higher than that of the Control sample found in this study (198.2 kJ·mol^{-1}). This may be attributed to the differences in biomass properties, TG operating conditions, and heating rates.

Based on the results of fitted kinetic parameters, the pretreatments had altered the characteristics of the biomass samples and increased the activation energy [63]. It can be observed that the E_a values derived from all models for Control, AC, and ACTO samples varied with the degree of conversion. This variance could be linked to the complex interaction mechanism of biomass constituents with different pretreatments. Ceylan and Topcu [66] reported that the E_a value was proportional to the cellulose content in the biomass. In a separate study, Xiao et al. [65] reported that lignin content was responsible for the high value of E_a. However, the cellulose and lignin may have inconsistent impacts on E_a due to a large number of complex reactions which may occur in the pyrolysis process [67]. Furthermore, it was reported that other factors may have influence on the activation energies, such as micro-spatial variability of the hydrogen-bond network of cellulose, hemicellulose, and the covalent bonds between lignin and hemicellulose [68].

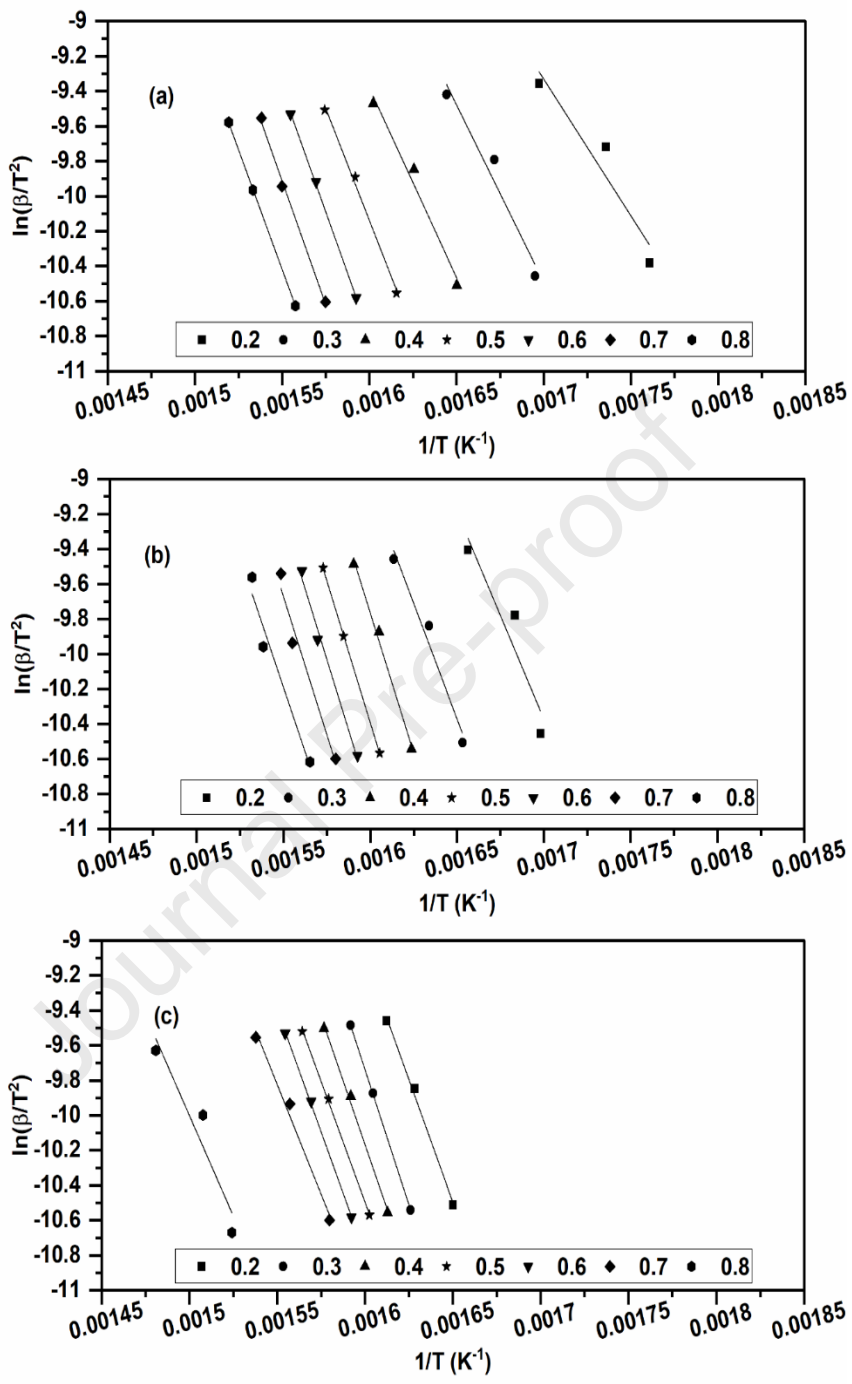

Fig. 5. Plots of ln(β/T^2) against 1/T for determination of kinetic parameters using DAEM method for: (a) Control sample; (b) AC biomass; and (c) ACTO biomass at a degree of conversion from 0.2 to 0.8.

The values of pre-exponential factor (*A*) derived from KAS, FWO, and DAEM models were found to be in the range of 1.5×10^{6}–9.6×10^{18} s^{-1}, 7.7×10^{8}–2.0×10^{22} s^{-1}, and 3.5×10^{9}–2.0×10^{23} s^{-1} for Control, AC, and ACTO samples, respectively. Generally, the *A* value increases with the presence of pretreatment, and this is confirmed by other studies on pyrolysis of pinewood which showed increased *A* values from 7.0×10^{11} to 1.3×10^{12} s^{-1} with biomass torrefaction [23]. The substantial variability in the derived parameter values represent the complex composition of biomass samples and the complex reactions occurring in the decomposition [63].

Fig. 6 depicts the effects of degree of conversion on the activation energy during pyrolysis of Control, AC, and ACTO samples. It can be seen that the E_a values varied with the degree of conversion, and trend of E_a of the treated samples is distinct from that of the Control sample. This was largely due to the influence of pretreatment on the pyrolysis process, which consists of parallel and competitive reactions [21]. Furthermore, the E_a values are also affected by the kinetic model employed. As expected, the activation energies obtained by the Kissinger method were relatively constant with the degree of conversion. Therefore, the detailed kinetic mechanism was unable to be obtained from this method [33]. The variation of activation energy with respect to the degree of conversion is linked to the component matrix and interconnections of components of the sample upon pretreatment. As a result, every treated sample represents unique decomposition characteristics owing to the pretreatment effects on individual components.

At a lower degree of conversion, hemicellulose and cellulose are prone to thermal cracking indicated by initial increase in the *Ea* value. Lignin is more stable, thus decomposes over a broad range of temperatures at higher conversion values. For the ACTO

sample, the decomposition of cellulose and hemicellulose occurred in shorter conversion interval of 0.2-2–0.3 with high E_a values. The pyrolysis process started with cellulose decomposition at higher activation energy than hemicellulose. On the other hand, Control and AC samples showed higher interval of 0.2-2–0.4 and 0.2-2–0.7, respectively, for the decomposition of cellulose and hemicellulose.

The mean values of E_a by KAS method for Control, AC, and ACTO were 190.1 kJ·mol^{-1}, 237.6 kJ·mol^{-1}, and 227.8 kJ·mol^{-1}, respectively. For FWO method, the mean value of E_a increased to 197.1 kJ·mol^{-1}, 245.7 kJ·mol^{-1}, and 228.3 kJ·mol^{-1}, while the corresponding E_a values from DAEM method were 198.2 kJ·mol^{-1}, 246.9 kJ·mol^{-1}, and 227.8 kJ·mol^{-1}, respectively. The mean E_a values obtained from KAS, FWO, and DAEM techniques further confirm that pyrolysis of combined chemically and torrefied biomass samples required more energy than Control and solely chemically treated samples. This is largely attributed to the low volatile matter and high fixed carbon as retained in ACTO sample.

As observed in Fig. 6, the activation energy values peaked at a range of 0.6 to 0.7 for the degree of conversion for Control and AC samples, and at approximately 0.3 for the ACTO sample. These results could be linked to the transformation derived from the decomposition of cellulose and hemicellulose to the decomposition of lignin [61]. As previously discussed, the mean activation energy derived from KAS, FWO, and DAEM models were close, with discrepancies of less than 10%, as presented in Table 4 [23].

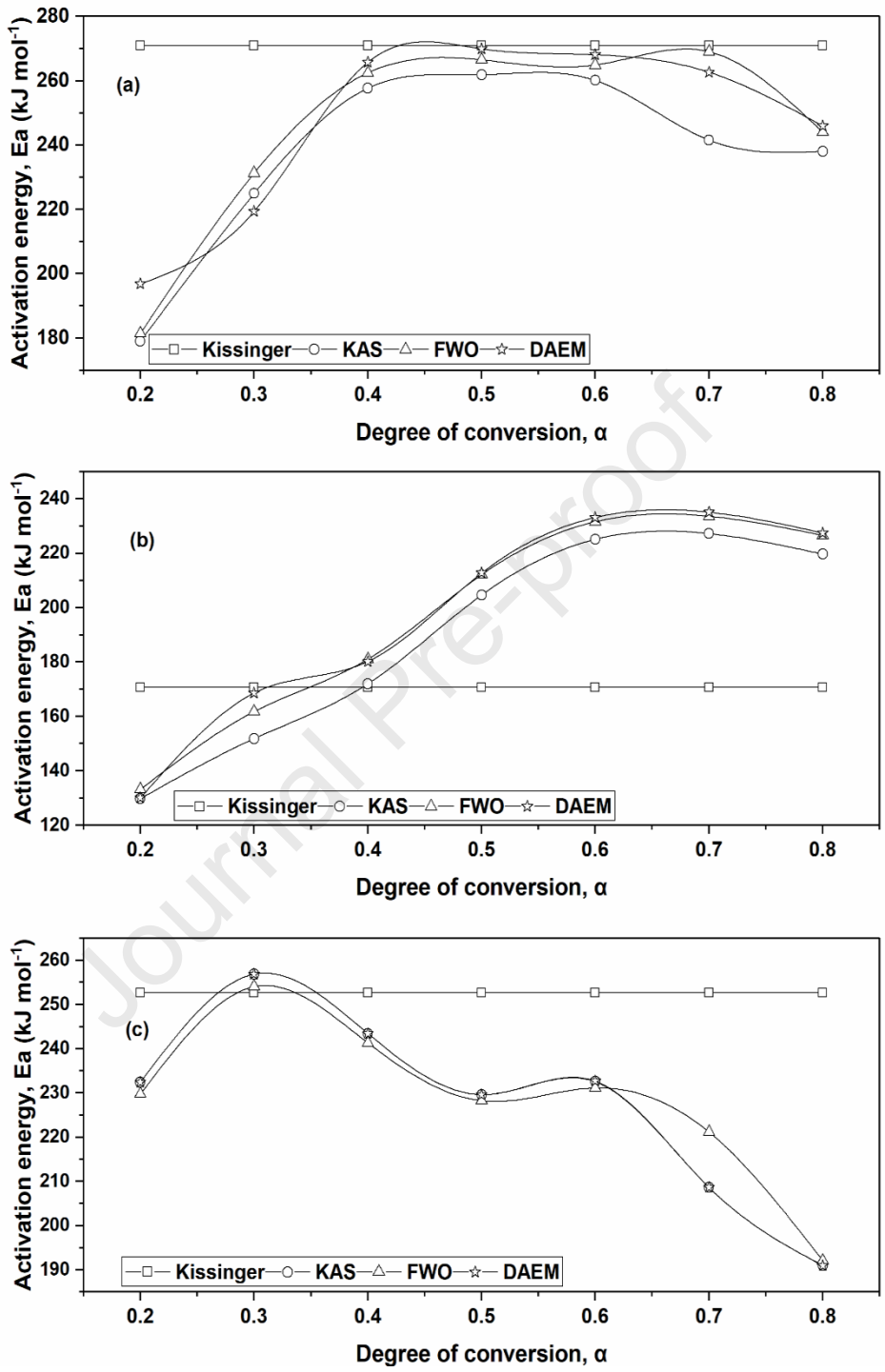

554

555 **Fig. 6.** Activation energy derived from Kissinger, KAS, FWO, and DAEM methods as a

556 function of degree of conversion for (a). Control; (b). AC biomass and (c) ACTO biomass.

4.0 Conclusions

Biomass of radiata pine was treated by chemical, torrefaction, and combined methods. The pyrolysis kinetics of the treated radiate pine were initially investigated by adopting Kissinger, KAS, FWO, and DAEM models on TG analysis results. It was found that after pretreatments, some components of the biomass underwent degradation, thereby changing the properties of the biomass, which would affect the thermal degradation behaviour and pyrolysis kinetic parameters. Overall, the activation energy, E_a, in the pyrolysis of the treated biomass increased over the degree of conversion from 0.2 to 0.8. The high E_a values indicate slower pyrolysis reactions, which can be explained by the chemical and compositional changes based on the ultimate and proximate analyses.

Moreover, the increased value of E_a could be explained by the high crystallinity after chemical pretreatment, and the cross-linking and carbonisation effects by torrefaction pretreatment. The E_a values varied with different pretreatment methods, indicating a complex multi-step mechanism and different degradation paths during pyrolysis of the treated biomasses. The pre-exponential factor, A, was found to be positively correlated to E_a attributing to the changes of active components of the biomass, dominantly, the cellulose. The A values obtained by KAS and FWO models were lower than the values obtained by DAEM model, indicating the dependency of mathematical formulation. These kinetic parameters allow for an improved understanding of the complex mechanisms of pyrolysis reaction of radiate pine biomass subjected to chemical and torrefaction pretreatments.

Appendix A. Supplementary data

E-supplementary data of this work can be found in an online version of the paper.

Acknowledgements

The authors thanks University of Canterbury, New Zealand and Universiti Teknologi MARA, Malaysia for financial support.

References

[1] S.I. Mussatto, Chapter 8 - Biomass pretreatment with acids, in: S.I. Mussatto (Ed.), Biomass fractionation technologies for a lignocellulosic feedstock based biorefinery, Elsevier, Amsterdam, 2016, pp. 169-185.

[2] T. Kan, V. Strezov, T.J. Evans, Lignocellulosic biomass pyrolysis: A review of product properties and effects of pyrolysis parameters, Renewable and Sustainable Energy Reviews, 57 (2016) 1126-1140.

[3] O. Das, A.K. Sarmah, Mechanism of waste biomass pyrolysis: Effect of physical and chemical pre-treatments, Sci. Total Environ., 537 (2015) 323-34.

[4] T. Wigley, A.C.K. Yip, S. Pang, Pretreating biomass via demineralisation and torrefaction to improve the quality of crude pyrolysis oil, Energy, 109 (2016) 481-494.

[5] C.D. Blasi, C. Branca, A. Galgano, Effects of diammonium phosphate on the yields and composition of products from wood pyrolysis, Ind. Eng. Chem. Res., 46 (2007) 430-438.

[6] Y. Hu, S. Wang, Q. Wang, Z. He, X. Lin, S. Xu, H. Ji, Y. Li, Effect of different pretreatments on the thermal degradation of seaweed biomass, Proc. Combust. Inst., 36 (2) (2017) 2271-2281.

603 [7] Y. Chen, M.A. Stevens, Y. Zhu, J. Holmes, H. Xu, Understanding of alkaline pretreatment
604 parameters for corn stover enzymatic saccharification, Biotechnol. Biofuels, 6 (8) (2013).
605 [8] J.S. Kim, Y.Y. Lee, T.H. Kim, A review on alkaline pretreatment technology for bioconversion
606 of lignocellulosic biomass, Bioresour. Technol., 199 (2016) 42-8.
607 [9] H. Wang, R. Srinivasan, F. Yu, P. Steele, Q. Li, B. Mitchell, Effect of acid, alkali, and steam
608 explosion pretreatments on characteristics of bio-oil produced from pinewood, Energy Fuels, 25 (8)
609 (2011) 3758-3764.
610 [10] I.Y. Mohammed, Y.A. Abakr, F.K. Kazi, S. Yusuf, Effects of pretreatments of napier grass
611 with deionized water, sulfuric acid and sodium hydroxide on pyrolysis oil characteristics, Waste
612 Biomass Valorization, 8 (3) (2017) 755-773.
613 [11] V.S. Chang, M.T. Holtzapple, Fundamental factors affecting biomass enzymatic reactivity,
614 Appl. Biochem. Biotechnol., 84 (1) (2000) 5-37.
615 [12] Hemansi, R. Gupta, V.K. Aswal, J.K. Saini, Sequential dilute acid and alkali deconstruction of
616 sugarcane bagasse for improved hydrolysis: Insight from small angle neutron scattering (SANS),
617 Renew. Energ., 147 (2020) 2091-2101.
618 [13] M.H. Tsai, W.C. Lee, W.C. Kuan, S. Sirisansaneeyakul, A. Savarajara, Evaluation of different
619 pretreatments of Napier grass for enzymatic saccharification and ethanol production, Energy Sci.
620 Eng., 6 (6) (2018) 683-692.
621 [14] S. Zhang, Y. Su, D. Xu, S. Zhu, H. Zhang, X. Liu, Effects of torrefaction and organic-acid
622 leaching pretreatment on the pyrolysis behavior of rice husk, Energy, 149 (2018) 804-813.
623 [15] M.A. Martín-Lara, G. Blázquez, M.C. Zamora, M. Calero, Kinetic modelling of torrefaction of
624 olive tree pruning, Appl. Therm. Eng., 113 (2017) 1410-1418.
625 [16] S. Ukaew, J. Schoenborn, B. Klemetsrud, D.R. Shonnard, Effects of torrefaction temperature
626 and acid pretreatment on the yield and quality of fast pyrolysis bio - oil from rice straw, J. Anal.
627 Appl. Pyrolysis, 129 (2018) 112-122.

628 [17] T. Wigley, A.C.K. Yip, S. Pang, A detailed product analysis of bio-oil from fast pyrolysis of
629 demineralised and torrefied biomass, J. Anal. Appl. Pyrolysis, 123 (2017) 194-203.
630 [18] T. Wigley, A.C.K. Yip, S. Pang, The use of demineralisation and torrefaction to improve the
631 properties of biomass intended as a feedstock for fast pyrolysis, J. Anal. Appl. Pyrolysis, 113
632 (2015) 296-306.
633 [19] V. Dhyani, T. Bhaskar, Kinetic analysis of biomass pyrolysis, Waste Biorefinery2018, pp. 39-
634 83.
635 [20] G. Mishra, J. Kumar, T. Bhaskar, Kinetic studies on the pyrolysis of pinewood, Bioresour.
636 Technol., 182 (2015) 282-288.
637 [21] L. Wang, H. Lei, J. Liu, Q. Bu, Thermal decomposition behavior and kinetics for pyrolysis and
638 catalytic pyrolysis of Douglas fir, RSC Adv., 8 (4) (2018) 2196-2202.
639 [22] E.G. Díaz, E. González, M.F. García, I.A. Asensio, Kinetic study of the pyrolysis of canary
640 pine: The relationship between the elemental composition and the kinetic parameters, Ind. Eng.
641 Chem. Res., 57 (28) (2018) 9094-9101.
642 [23] Q. He, L. Ding, Y. Gong, W. Li, J. Wei, G. Yu, Effect of torrefaction on pinewood pyrolysis
643 kinetics and thermal behavior using thermogravimetric analysis, Bioresour. Technol., 280 (2019)
644 104-111.
645 [24] A.K. Varma, P. Mondal, Physicochemical characterization and kinetic study of pine needle for
646 pyrolysis process, J. Therm. Anal. Calorim., 124 (1) (2015) 487-497.
647 [25] J. Zhang, J. Gu, H. Yuan, Y. Chen, Thermal behaviors and kinetics for fast pyrolysis of
648 chemical pretreated waste cassava residues, Energy, 208 (2020).
649 [26] R.M. Braga, T.R. Costa, J.C.O. Freitas, J.M.F. Barros, D.M.A. Melo, M.A.F. Melo, Pyrolysis
650 kinetics of elephant grass pretreated biomasses, J. Therm. Anal. Calorim., 117 (3) (2014) 1341-
651 1348.

652 [27] X. Tian, L. Dai, Y. Wang, Z. Zeng, S. Zhang, L. Jiang, X. Yang, L. Yue, Y. Liu, R. Ruan,
653 Influence of torrefaction pretreatment on corncobs: A study on fundamental characteristics, thermal
654 behavior, and kinetic, Bioresour. Technol., 297 (2020) 122490.
655 [28] B.-H. Lee, T.-Y. Jeong, V.T. Trinh, C.-H. Jeon, Thermal degradation of kenaf (Hibiscus
656 cannabinus L.): Impact of torrefaction on pyrolysis kinetics and thermal behavior, Energy Reports,
657 7 (2021) 951-959.
658 [29] S. Zhang, Y. Su, Y. Xiong, Influence of coupling demineralization with the torrefaction
659 pretreatment process on the pyrolysis characteristics and kinetics of rice husk, Energy Sources, Part
660 A: Recovery, Utilization and Environmental Effects, 39 (7) (2017) 726-732.
661 [30] N.N. Kasim, K. Ismail, A.R. Mohamed, M.A.M. Ishak, R. Ahmad, W. Ismail, Characteristic,
662 thermochemical behaviors and kinetic of demineralized and torrefied empty fruit bunches (EFB),
663 Advances in Science, Technology and Engineering Systems, 3 (5) (2018) 365-373.
664 [31] A. Pimchuai, A. Dutta, P. Basu, Torrefaction of agriculture residue to enhance combustible
665 properties, Energy Fuels, 24 (9) (2010) 4638-4645.
666 [32] T. Wigley, Improving the quality of bio-oil by fast pyrolysis of acid leached and torrefied
667 Pinus radiata, Chemical and Process Engineering, University of Canterbury, 2015, p. 275.
668 [33] S. Vyazovkin, C.A. Wight, Model-free and model-fitting approaches to kinetic analysis of
669 isothermal and nonisothermal data, Thermochim. Acta, 340-341 (1999) 53-68.
670 [34] A.W. Coats, J.P. Redfern, Kinetic parameters from thermogravimetric data, Nature, 201
671 (1964) 68-69.
672 [35] Y.S. Kim, Y.S. Kim, S.H. Kim, Investigation of thermodynamic parameters in the thermal
673 decomposition of plastic waste-waste lube oil compounds, Environ. Sci. Technol., 44 (13) (2010)
674 5313-7.
675 [36] D. Viju, R. Gautam, R. Vinu, Application of the distributed activation energy model to the
676 kinetic study of pyrolysis of Nannochloropsis oculata, Algal Res., 35 (2018) 168-177.

677 [37] R.K. Mishra, K. Mohanty, Pyrolysis kinetics and thermal behavior of waste sawdust biomass
678 using thermogravimetric analysis, Bioresour. Technol., 251 (2018) 63-74.
679 [38] K. Miura, T. Maki, A simple method for estimating f(E) and k0(E) in the Distributed
680 Activation Energy Model, Energy Fuels, 12 (5) (1998) 864-869.
681 [39] M. Kashaninejad, L.G. Tabil, Effect of microwave–chemical pre-treatment on compression
682 characteristics of biomass grinds, Biosyst Eng, 108 (1) (2011) 36-45.
683 [40] S. Ramos-Carmona, J.F. Pérez, M.R. Pelaez-Samaniego, R. Barrera, M. Garcia-Perez, Effect of
684 torrefaction temperature on properties of Patula pine, Maderas: Ciencia y Tecnologia, 19 (1) (2017)
685 39-50.
686 [41] J.S. Tumuluru, Effect of deep drying and torrefaction temperature on proximate, ultimate
687 composition, and heating value of 2-mm lodgepole pine (Pinus contorta) grind, Bioengineering 3(2)
688 (2016).
689 [42] J. Park, J. Meng, K.H. Lim, O.J. Rojas, S. Park, Transformation of lignocellulosic biomass
690 during torrefaction, J. Anal. Appl. Pyrolysis, 100 (2013) 199-206.
691 [43] S. Kanwal, N. Chaudhry, S. Munir, H. Sana, Effect of torrefaction conditions on the
692 physicochemical characterization of agricultural waste (sugarcane bagasse), Waste Manage., 88
693 (2019) 280-290.
694 [44] L. Jiang, S. Hu, L.S. Sun, S. Su, K. Xu, L.M. He, J. Xiang, Influence of different
695 demineralization treatments on physicochemical structure and thermal degradation of biomass,
696 Bioresour. Technol., 146 (2013) 254-60.
697 [45] V. Savou, G. Grause, S. Kumagai, Y. Saito, T. Kameda, T. Yoshioka, Pyrolysis of sugarcane
698 bagasse pretreated with sulfuric acid, J. Energy Inst., 92 (4) (2019) 1149-1157.
699 [46] Z. Chen, Q. Zhu, X. Wang, B. Xiao, S. Liu, Pyrolysis behaviors and kinetic studies on
700 Eucalyptus residues using thermogravimetric analysis, Energy Convers. Manag., 105 (2015) 251-
701 259.

[47] A. Saffe, A. Fernandez, G. Mazza, R. Rodriguez, Prediction of regional agro-industrial wastes characteristics by thermogravimetric analysis to obtain bioenergy using thermal process, Energy Explor. Exploit., 37 (1) (2018) 544-557.

[48] A. Zheng, K. Zhao, L. Li, Z. Zhao, L. Jiang, Z. Huang, G. Wei, F. He, H. Li, Quantitative comparison of different chemical pretreatment methods on chemical structure and pyrolysis characteristics of corncobs, Journal of the Energy Institute, 91 (2018) 676-682.

[49] H. Yang, R. Yan, H. Chen, D.H. Lee, C. Zheng, Characteristics of hemicellulose, cellulose and lignin pyrolysis, Fuel, 86 (12-13) (2007) 1781-1788.

[50] H. Yang, R. Yan, H. Chen, C. Zheng, D.H. Lee, D.T. Liang, In-depth investigation of biomass pyrolysis based on three major components hemicellulose, cellulose and lignin, Energy Fuels, 20 (2006) 388-393.

[51] E. Menya, P.W. Olupot, H. Storz, M. Lubwama, Y. Kiros, M.J. John, Effect of alkaline pretreatment on the thermal behavior and chemical properties of rice husk varieties in relation to activated carbon production, J. Therm. Anal. Calorim., 139 (3) (2019) 1681-1691.

[52] I.-Y. Eom, J.-Y. Kim, T.-S. Kim, S.-M. Lee, D. Choi, I.-G. Choi, J.-W. Choi, Effect of essential inorganic metals on primary thermal degradation of lignocellulosic biomass, Bioresour. Technol., 104 (2012) 687-694.

[53] F. Pardo, L. M., S. Mendoza, J. G., L. Galán, J. E., Influence of pretreatments on crystallinity and enzymatic hdrolysis in sugar cane residues, Brazilian Journal of Chemical Engineering, 36 (1) (2019) 131-141.

[54] M. Asadieraghi, W.M.A. Wan Daud, Characterization of lignocellulosic biomass thermal degradation and physiochemical structure: Effects of demineralization by diverse acid solutions, Energy Convers. Manag, 82 (2014) 71-82.

[55] S. Zhou, Y. Xue, J. Cai, C. Cui, Z. Ni, Z. Zhou, An understanding for improved biomass pyrolysis: Toward a systematic comparison of different acid pretreatments, Chem. Eng. J., 411 (2021).

[56] M.A. Javed, Acid treatment effecting the physiochemical structure and thermal degradation of biomass, Renewable Energy, 159 (2020) 444-450.

[57] Z. Sebestyén, Z. May, K. Réczey, E. Jakab, The effect of alkaline pretreatment on the thermal decomposition of hemp, J. Therm. Anal. Calorim., 105 (3) (2010) 1061-1069.

[58] C. Diblasi, Modeling chemical and physical processes of wood and biomass pyrolysis, Prog. Energy Combust. Sci., 34 (1) (2008) 47-90.

[59] A.G. Bradbury, Y. Sakai, F. Shafizadeh, A kinetic model for pyrolysis of cellulose, J. Appl. Polym. Sci., 23 (11) (1979) 3271-3280.

[60] R. Liu, J.J. Morrell, L. Yan, Thermogravimetric analysis studies of thermally-treated glycerol impregnated poplar wood, Bioresources, 13 (1) (2018) 1563-1575.

[61] F. Rego, A.P. Soares Dias, M. Casquilho, F.C. Rosa, A. Rodrigues, Pyrolysis kinetics of short rotation coppice poplar biomass, Energy, (2020).

[62] S. Singh, A.N. Sawarkar, Thermal decomposition aspects and kinetics of pyrolysis of garlic stalk, Energy Sources, Part A: Recovery, Utilization, and Environmental Effects, 0 (0) (2020) 1-11.

[63] R. Kaur, P. Gera, M.K. Jha, T. Bhaskar, Pyrolysis kinetics and thermodynamic parameters of castor (Ricinus communis) residue using thermogravimetric analysis, Bioresour. Technol., 250 (2018) 422-428.

[64] Z. Ma, D. Chen, J. Gu, B. Bao, Q. Zhang, Determination of pyrolysis characteristics and kinetics of palm kernel shell using TGA–FTIR and model-free integral methods, Energy Convers. Manag., 89 (2015) 251-259.

[65] R. Xiao, W. Yang, X. Cong, K. Dong, J. Xu, D. Wang, X. Yang, Thermogravimetric analysis and reaction kinetics of lignocellulosic biomass pyrolysis, Energy, 201 (2020) 117537.

[66] S. Ceylan, Y. Topcu, Pyrolysis kinetics of hazelnut husk using thermogravimetric analysis, Bioresour. Technol., 156 (2014) 182-8.

[67] M. Radojevic, B. Jankovic, V. Jovanovic, D. Stojiljkovic, N. Manic, Comparative pyrolysis kinetics of various biomasses based on model-free and DAEM approaches improved with numerical optimization procedure, PLoS One, 13 (10) (2018) e0206657.

[68] J.D. Murillo, J.J. Biernacki, S. Northrup, A.S. Mohammad, Biomass pyrolysis kinetics: A review of molecular-scale modeling contributions, Brazilian J. Chem. Eng., 34 (1) (2017) 1-18.